Statistical Analysis of Sea-Clutter using K-Pareto, K-CGIG, and Pareto-CGIG Combination Models with Noise

HOUCINE OUDIRA[1*], MEZACHE AMAR[2], AMEL GOURI[3]
[1]LGE Laboratory university of M'Sila,
Department of Electronics,
University Mohamed Boudiaf of M'Sila,
ALGERIA

[2]SISCOM Laboratory university of M'Sila,
Department of Electronics,
University Mohamed Boudiaf of M'Sila,
ALGERIA

[3]LASS Laboratory university of M'Sila
Department of Electronics,
University Mohamed Boudiaf of M'Sila,
ALGERIA

**Corresponding Author*

Abstract: - In this paper, the combinations of two compound Gaussian distributions plus thermal noise for modeling measured polarimetric clutter data are proposed. The speckle components of the proposed models are formed by the exponential distribution, while the texture components are mainly modeled using three different distributions. For this purpose, the gamma, the inverse gamma, and the inverse Gaussian distributions are considered to describe these modulation components. The study involves the analysis of underlying mixture models at X-band sea clutter data, and the parameters of the combination models are estimated using the non-linear least squares curve fitting method. Compared to existing K, Pareto type II, and KK clutter plus noise distributions, experimental results show that the proposed mixture models are well matched for fitting sea reverberation data across various range resolutions.

Key-Words: - Combination models, Nelder-Mead algorithm, Sea clutter, Random textures, speckle, Noise.

Received: July 6, 2022. Revised: October 16, 2023. Accepted: November 19, 2023. Published: December 27, 2023.

1 Introduction

In radar systems with low resolution capabilities, the intensity statistics of the sea echoes have been found to be described by the exponential (i.e., Gaussian clutter case) probability density function (PDF). With the development of radar technologies operating at low grazing angles, the resolutions of sea clutter statistics have been greatly reduced and have been observed to deviate from Gaussianity, [1]. Consequently, these deviations occur when the Central Limit Theorem does not apply in evaluating the strength of the background electromagnetic energy (i.e., when independent random variables are added, their sum does not tends toward a normal distribution). Nowadays, compound Gaussian (CG) distributions are commonly used to fit high-resolution sea reverberation data and are the basis of the construction of most target detection schemes with CFAR (Constant False Alarm Rate) behavior, [2]. The CG models are formed by means of two components; the speckle component and the texture component that is also termed by the modulation component. In the sense of tail fitting improvements to high-resolution real data, some distributions related to the texture component have been proposed in the open literature, [3], [4], [5], [6], [7]. The inverse gamma and the inverse Gaussian distributed texture components were used to obtain the generalized Pareto (GP) and the compound Gaussian inverse Gaussian (CGIG) PDFs respectively, [3], [4]. These models have been effectively tested to fit the McMaster Intelligent Pixel Processing (IPIX) radar lake-clutter measurements and are extended to incorporate the

thermal (system) noise in order to attaint better goodness-of-fit against the Weibull, Log-normal and K distributions, [5], [6]. Compared to the standard Pareto model, the fractional order Pareto distribution was shown to produce excellent fits to the Defence Science Technology Organization (DSTO) Ingara data collected by X-band maritime surveillance radar, [7]. Another way to obtain the best fitting to empirical data is to use the mixture models, i.e., the mixture of two or more distributions. In this context, the KK distribution is applied for the analysis of the Ingara data collected at medium to high grazing angles, [8]. The model is generalized to account the addition of multiple looks and a thermal noise component to produce greater accuracy of the underlying shape of the fitted PDF. The required detection threshold to achieve a constant false alarm rate was also studied and compared with the K-distribution. [9], proposed a mixture of a Rayleigh and a K PDFs for representing active sonar data comprising clutter sparsely observed in a Rayleigh-distributed background. The K-Rayleigh mixture was seen to provide improved PDF fits and inference on the clutter statistics. A parameter estimation technique based on the expectation maximization (EM) algorithm is proposed and shown to perform adequately, [9]. The reference, [10], proposed an alternative statistical model, which is a mixture of *K*-distribution and log-normal distribution for modeling the SAR (synthetic aperture radar) data. This mixture model is able to model the clutter data, the target data, or the mixed data of clutter and target. The flowchart of the maximum likelihood (ML) method using the EM approach was presented for estimating the respective parameters of the proposed mixture model.

In this paper, the modelling of sea radar clutter using a mixture of two compound Gaussian distributions plus thermal noise is presented. The speckle component of the proposed models is formed by an exponential distribution where the texture components are particularly modelled by means of two different distributions, [11]. The work presented in, [11], is extended in this paper to account three mixture models which are compared to the K, GP and KK clutter plus noise models. To do this, the gamma, the inverse gamma and the inverse Gaussian distributions are considered to describe the modulation components. The proposed models are analysed and the non-linear least squares curve fitting technique based on the Nelder-Mead algorithm, [12], is employed to obtain the optimal parameter estimation. Compared to the existing KK, K, and Pareto clutter plus noise distributions, experimental results show that the proposed mixture models with different random textures are well suited to fit high resolution sea clutter data in most cases. This paper is structured in the following manner. In section 2, we briefly recall the expressions of the K, the Pareto and the CIG (compound inverse Gaussian) clutter plus noise PDFs. Section 3 describes the proposed mixture models where the flowchart of the the N-M algorithm is presented. Section 4 investigates modeling comparisons using IPIX data of the proposed mixture models against the existing K, GP and KK distributions plus noise. Finally, main concluding remarks are listed in section 5.

2 Review of K, Pareto and CIG plus Noise Distribution

This section introduces compound Gaussian processes for characterizing sea-clutter returns, which are composed of a rapidly fluctuating speckle component influenced by a slowly fluctuating texture component. Assuming independent and identically distributed (iid) single look data, the combined CG distribution of the random variable X is described as per reference, [1].

$$p_X(x) = \int_0^\infty p_{X|Y}(x|y)\, p_Y(y) dy \tag{1}$$

If a square law detector is used and the thermal noise power denoted by $p_n = 2\sigma^2$ is incorporated, the speckle component (namely the conditional PDF of x given y) follows the exponential distribution (i.e., single pulse case) given by:

$$p_{X|Y}(x|y) = \frac{1}{y + p_n} \exp\left(-\frac{x}{y + p_n} \right) \tag{2}$$

The *K*-distribution plus noise is obtained if the texture component fluctuates according to a gamma PDF, [2].

$$p_Y(y) = \frac{b^\nu y^{\nu-1}}{\Gamma(\nu)} \exp(-by) \tag{3}$$

where ν is the shape parameter which governs the spikness of the clutter, b is the scale parameter and $\Gamma(.)$ is the gamma function. Substituting (2) and (3) into (1), the overall *K* plus noise PDF is given in integral form, [13], [14].

$$p_X(x) = \frac{b^\nu}{\Gamma(\nu)} \int_0^\infty \frac{y^{\nu-1}}{y + p_n} \exp\left(-\frac{x}{y + p_n} \right) \exp(-by) dy \tag{4}$$

The complementary cumulative distributed function (CCDF) related to (4) is:

$$CCDF = \frac{b^{\nu}}{\Gamma(\nu)}\int_0^{\infty} y^{\nu-1}\exp\left(-\frac{T}{p_n+y}\right)\exp(-by)dy \quad (5)$$

where T denotes the normalized detection threshold. It is shown in, [14], that the moment formula of order $r>0$ can be expressed as

$$\langle x^r\rangle = p_n^r\Gamma(r+1)\,{}_2F_0\left(\nu,-r;.;-\frac{1}{bp_n}\right) \quad (6)$$

where ${}_2F_0(.,.;.;)$ is the generalized hyergeometric function.

When the modulation component is an inverse gamma PDF, the Pareto plus noise distribution is constructed, [3], [15].

$$p_Y(y) = \frac{\beta^{\alpha}y^{-\alpha-1}}{\Gamma(\alpha)}\exp\left(-\frac{\beta}{y}\right) \quad (7)$$

Where α is the shape parameter which depends on heavy tailed clutter and b is the scale parameter. Substituting (2) and (7) into (1), the Pareto plus noise PDF is obtained, [16], [17].

$$p_X(x) = \frac{\beta^{\alpha}}{\Gamma(\alpha)}\int_0^{\infty}\frac{y^{-\alpha-1}}{p_n+y}\exp\left(-\frac{x}{p_n+y}\right)\exp\left(-\frac{\beta}{y}\right)dy \quad (8)$$

Integrating (8) from T to $+\infty$, the corresponding CCDF is also given in an integral form:

$$CCDF = \frac{\beta^{\alpha}}{\Gamma(\alpha)}\int_0^{\infty} y^{-\alpha-1}\exp\left(-\frac{T}{p_n+y}\right)\exp\left(-\frac{\beta}{y}\right)dy \quad (9)$$

Using (8), the expression of moments of order $r<\alpha$ is derived in, [17], to be:

$$\langle x^r\rangle = \frac{\beta^r\Gamma(1+r)\Gamma(\alpha-r)}{\Gamma(\alpha)}\,{}_2F_0\left(\alpha-r,-r;;-\frac{p_n}{\beta}\right) \quad (10)$$

If the inverse Gaussian law is used to describe the modulation component in (1), the CIG plus noise PDF is obtained. The underlying inverse Gaussian distribution is presented in, [18], [19].

$$p_Y(y) = \frac{\lambda^{1/2}}{\sqrt{2\pi}y^{3/2}}\exp\left(-\lambda\frac{(y-\mu)^2}{2\mu^2 y}\right) \quad (11)$$

Where λ is the shape parameter and μ is the mean. Note that, λ relies upon sea conditions and radar parameters. Spiky clutter corresponds to values of $0<\lambda<1$ and the Exponential distribution or Gaussian clutter is attained for $\lambda\to\infty$. Substituting (2) and (11) into (1), the CIG PDF plus noise is expressed by:

$$p_X(x) = \frac{\lambda^{1/2}}{\sqrt{2\pi}}\int_0^{\infty}\frac{y^{-3/2}}{y+p_n}\exp\left(-\frac{x}{y+p_n}\right)\exp\left(-\lambda\frac{(y-\mu)^2}{2\mu^2 y}\right)dy \quad (12)$$

The corresponding CCDF of (12) is determined to be:

$$CCDF = \frac{\lambda^{1/2}}{\sqrt{2\pi}}\int_0^{\infty} y^{-3/2}\exp\left(-\frac{T}{p_n+y}\right)\exp\left(-\lambda\frac{(y-\mu)^2}{2\mu^2 y}\right)dy \quad (13)$$

Contrary of (6) and (10), it is difficult to solve the integral of moment's expression from (12) of order r. Numerical integration is used to evaluate the following non-integer order moments

$$\langle x^r\rangle = \Gamma(1+r)\sqrt{\frac{\lambda}{2\pi}}e^{\lambda/\mu}\int_0^{\infty} y^{-3/2}(y+p_n)^r\exp\left(-\frac{\lambda}{2\mu^2}y-\frac{\lambda}{2y}\right)dy \quad (14)$$

3 Proposed Combination of CG Models

In this section, mixtures CG models are presented with different random textures for the best tail fitting to real data. Three texture components are considered as devoted in Section 2. To this end, we resort to combine two CG distributions with an appropriate weighting factor k ($0<k<1$) given by, [10].

$$p(x) = kp_1(x|\theta_1) + (1-k)p_2(x|\theta_2) \quad (15)$$

where $\theta = [k,\theta_1,\theta_2]$ is a vector of unknown parameters to be estimated at each estimation task. The two CG distributions $p_1(x)$ and $p_2(x)$ have the same exponential distribution for the speckle component given by (2) and two different texture components. For instance, if we choose the CIG and the Pareto plus noise models to describe $p_1(x)$ and $p_2(x)$ respectively, (15) becomes (after substitution (8) and (12) into (15)).

$$p_X(x) = k\frac{\lambda^{1/2}}{\sqrt{2\pi}}\int_0^{\infty}\frac{y^{-3/2}}{y+p_n}\exp\left(-\frac{x}{y+p_n}\right)\exp\left(-\lambda\frac{(y-\mu)^2}{2\mu^2 y}\right)dy + \frac{(1-k)\beta^{\alpha}}{\Gamma(\alpha)}\int_0^{\infty}\frac{y^{-\alpha-1}}{p_n+y}\exp\left(-\frac{x}{p_n+y}\right)\exp(-\beta/y)dy \quad (16)$$

Note that (16) spans from CIG plus noise PDF to Pareto plus noise PDF. With k=1 and k=0 corresponding to the purely CIG plus noise distribution and the purely Pareto plus noise distribution respectively. If $0<k<1$, (16) is a mixture of the CIG and the Pareto plus noise PDFs. Consequently, several combinations between K+noise, Pareto+noise and CIG+noise PDFs can be used in (15). However, it is shown in, [12], that the best estimation of the parameters of K-clutter plus noise model can be achieved when the corresponding CCDF is used in the objective or fitness function of the N-M algorithm. To this effect, we apply in this work the PCFE (parametric curve fitting estimation) method described in, [11], [12], to optimize the parameters of the following

CCDFs instead of mixture models used in (15). In the case of the CCDF obtained from a mixture of the CIG and Pareto plus noise models, it is easy to obtain:

$$CCDF_{Pareto}^{CIG} = k\frac{\lambda^{1/2}}{\sqrt{2\pi}}\int_0^{\infty} y^{-3/2}\exp\left(-\frac{T}{y+p_n}\right)\exp\left(-\lambda\frac{(y-\mu)^2}{2\mu^2 y}\right)dy + \frac{(1-k)\beta^{\alpha}}{\Gamma(\alpha)}\int_0^{\infty} y^{-\alpha-1}\exp\left(-\frac{T}{p_n+y}\right)\exp(-\beta/y)dy \quad (17)$$

where $\theta = [k, \lambda, \mu, \alpha, b, p_n]$. The CCDF obtained from a mixture of CIG and *K* plus noise models is

$$CCDF_{K}^{CIG} = k\frac{\lambda^{1/2}}{\sqrt{2\pi}}\int_0^{\infty} y^{-3/2}\exp\left(-\frac{T}{y+p_n}\right)\exp\left(-\lambda\frac{(y-\mu)^2}{2\mu^2 y}\right)dy + \frac{(1-k)b^{\nu}}{\Gamma(\nu)}\int_0^{\infty} y^{\nu-1}\exp\left(-\frac{T}{y+p_n}\right)\exp(-by)dy \quad (18)$$

In this case, $\theta = [k, \lambda, \mu, \nu, b, p_n]$. Also, the resulting CCDF from a mixture of K and Pareto plus noise models is given by

$$CCDF_{Pareto}^{K} = k\frac{b^{\nu}}{\Gamma(\nu)}\int_0^{\infty} y^{\nu-1}\exp\left(-\frac{T}{y+p_n}\right)\exp(-by)dy + \frac{(1-k)\beta^{\alpha}}{\Gamma(\alpha)}\int_0^{\infty} y^{-\alpha-1}\exp\left(-\frac{T}{p_n+y}\right)\exp(-\beta/y)dy \quad (19)$$

where $\theta = [k, \nu, b, \alpha, c, p_n]$. In (17)-(19), we have six unknown parameters to be optimized. Due to this complexity of parameter estimation, the PCFE based on the N-M simplex search algorithm is used. The best fit is simply achieved by a direct comparison of the experimentally measured CCDF with a set of curves derived from the theoretical CCDF given by (17)-(19). Thus, the residual can be formulated, in our case, as the difference between the experimentally measured CCDF of the recorded data and the theoretical model. An adequate tail fitting regions of the theoretical CCDFs with real data are optimized by means of the N-M algorithm which is the best known algorithm for multidimensional unconstrained optimization without derivatives. After a sufficient number of iterations, the algorithm converges to the global minimum and outputs the numerical estimates of the parameters. From the flowchart of Figure 1, the following basic steps of the N-M algorithm are given below with fixed parameters, $\rho = 1,\ \chi = 2,\ \gamma = 1/2$ and $\sigma = 1/2$, [11].

Step 1: Estimate the real CCDF of the recorded data.

Step 2: Initialize the method.

Step 3: Calculate the initial working N–M simplex from the initial point given above.

Step 4: Evaluate the summed square of residuals between theoretical CCDFs with real data at each point (vertex) of the working N–M simplex.

Step 5: Repeat the following steps until the termination test is satisfied.

1 Calculate the termination test information.
2 If the termination test is satisfied then, accept the best vertex of the working N–M simplex and go to step 6, otherwise transform the working N–M simplex and go to step 4.

Step 6: Return the best point (vertex) of the working simplex Δ and the associated function value.

In the following section, the radar data that is used for sea clutter modeling is described. After that, the procedure to be followed for data analysis is provided.

4 Modeling Assessment using IPIX Data

The capabilities of the proposed mixture models given by (15) to fit the real PDFs and CCDFs given by (17-19) for various sets are investigated in this section. This modeling performance is assessed using real-world IPIX lake clutter. The lake-clutter data we processed were collected at Grimsby, Ontario, with the McMaster University IPIX radar. IPIX is an experimental X-band search radar, capable of dual polarized and frequency agile operation, [20]. As in reference, [4], we focus our analysis on the datasets 84, 85 and 86 which correspond to the range resolutions 30m, 15m and 3m respectively. The radar site was located at east of the "Place Polonaise" at Grimsby, Ontario (Latitude 43:2114±N, Longitude 79:5985±W), looking at lake Ontario from a height of 20 meter (m). The nearest shore on the far side of the lake is more than 20 Km away. The data of the Grimsby database are stored in 222 files, as 10 bits integers.

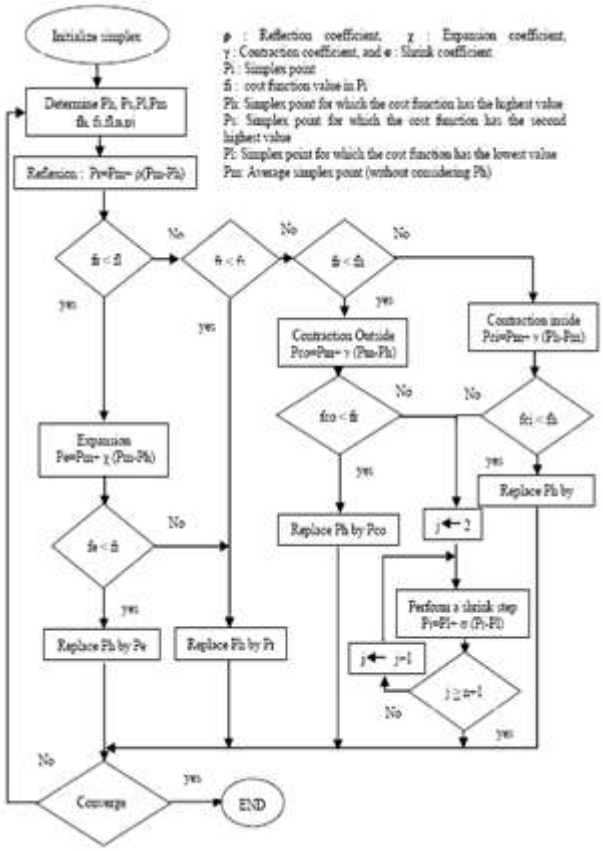

Fig. 1: Flowchart of the Nelder-Mead method

There are co-polarizations, HH and VV (Lpol), and cross-polarizations, HV and VH (Xpol), coherent reception, leading to a quadruplet of I and Q values for co-pol and cross-pol. Here, the experimental modeling analysis is carried out for HH and VV antenna polarizations, 3 m, 15 m and 30 m range cell resolutions. During the recordings, the radar was transmitting with a pulse-repetition frequency (PRF) of 1000 Hz and a pulse length of $0.06\,\mu s$. The received IPIX data is treated by the arrival order and registered in a (60000x34) matrix where 34 denotes the number of range cells and 60000 is the number of pulses. Because parameter estimation of compound Gaussian models cannot be obtained using low sample sizes, the proposed mixture models were validated using 60000 recorders rather than 34 range samples. High resolution sea clutter depends on both azimuth resolution which is related to the beam width and range resolution, ie., $d = c\tau/2$. In cases of d=3m, d=15m and d=30m, the pulse duration (i.e., sampling time) have three different values where the grazing angle is fixed at a low value. Thus, these data does not have a connection with the grazing angle.

In order to investigate the statistical properties of the data, we compare the empirical PDF and CCDF of the data with their theoretical mixture models in the case of single look data. Fitting with multilook data using for example 10 to 20 cells is not possible using the proposed theoretical distributions.

The tail fitting to real data is important in radar detection applications. Thus, 1000 independent samples are not sufficient to fit the tail of the corresponding PDFs and CCDFs. Usually, 10^5 samples are needed for a desired CCDF value of 10^{-3}. Each range cell, 60 000 measurements are therefore necessary to compare the tail fitting of the different models.

The following experimental procedure focuses firstly on the parameter estimation found by the N-M algorithm and secondly on the validation of the mixture models using the real data described previously. The MSE (Mea Square Error) values are calculated from the fitted and empirical CCDFs curves. According to these values which are obtained from specific range of the CCDFs between 10^{-3} and 10^{-2}, the proposed mixture models give lower values allowing best tail fitting as several scenes will show. The optimal estimates of the various models parameters as well as the MSE values are illustrated in Table 1 and Table 2. For HH polarization, resolution of 30m and 19th range cell, the PDFs and the CCDFs curves are depicted in Figure 2. It is clearly seen from this experiment that a mixture model constructed by the CIG plus *K* distributions provides the smallest value of MSE which means the best fit to empirical data. Now if the case of a resolution of 15m, a VV polarization is considered with 32th range cell, the theoretical mixture models CIG plus GP and K plus GP have quasi-similar results with the empirical CCDFs as shown in Figure 3. Next, we conduct the same test for a resolution of 3m, HH polarization, 17th range cell; better modeling performance is obtained by the K plus GP and CIG plus GP CCDFs as depicted in Figure 4. If another study based on the use of the same resolution with VV polarization and 9th range cell, Figure 5 illustrates the different PDFs and CCDFs for all considered models. In this experiment, it can also be seen that the tail of the proposed mixture models (CIG plus K and CIG plus GP) leads to the best fit. From these modelling experiments, it is pinpointed out that a mixture model constructed by the sum of the CIG, K, and GP distributions with noise is mostly an accurate statistical model of IPIX data, but it requires more computational time due to the number of estimated parameters.

Finally, the results obtained by the proposed mixture models are also assessed against those

obtained by the existing KK model with thermal noise, [8]. To this effect, we used the same PCFE based method given in Figure 1 to compute the KK clutter plus noise parameters. For this, the corresponding CCDF of the KK model with thermal noise is given by

$$CCDF_K^K = k\frac{b^{\nu}}{\Gamma(\nu)}\int_0^{\infty} y^{\nu-1}\exp\left(-\frac{T}{y+p_n}\right)\exp(-by)dy + (1-k)\frac{b^{\nu_1}}{\Gamma(\nu_1)}\int_0^{\infty} y^{\nu_1-1}\exp\left(-\frac{T}{y+p_n}\right)\exp(-by)dy \quad (20)$$

where $\theta = [k, \nu, b, \nu_1, b_1, p_n]$.

Table 3 illustrates the MSE values as well as the optimal estimates of the various models parameters. For VV polarization, resolution of 30m and 19th range cell, the PDFs and the CCDFs curves are depicted in Figure 6. It is clearly seen from this experiment that a mixture model constructed by the CIG plus GP distributions provides the smallest value of MSE which means the best fit to empirical data.

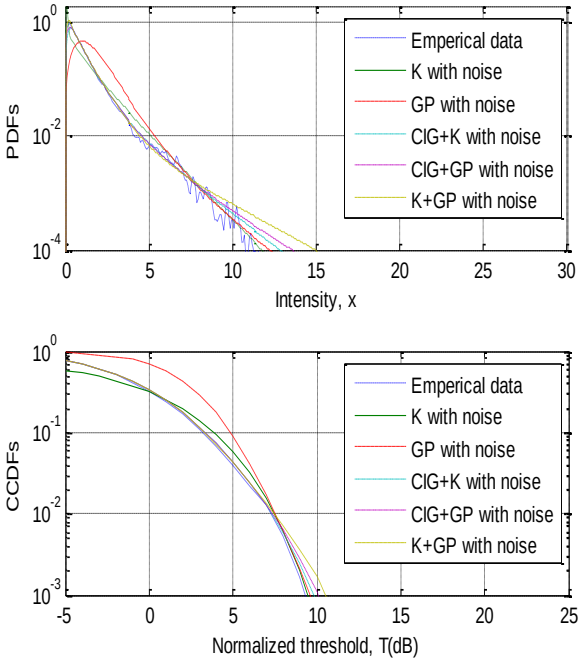

Fig. 2: Fitted PDFs and fitted CCDFs of mixture models for HH polarization, resolution of 30m and 19th range cell, dataset 84

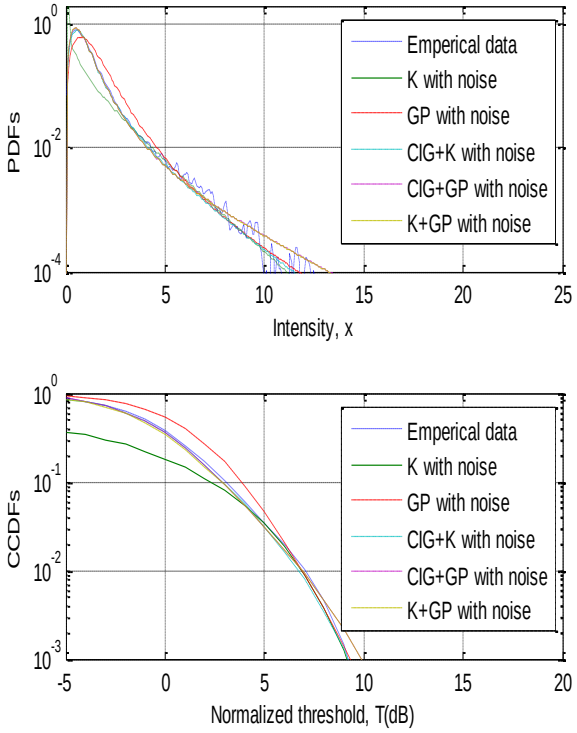

Fig. 3: Fitted PDFs and fitted CCDFs of mixture models for VV polarization, resolution of 15m and 32th range cell, dataset 85

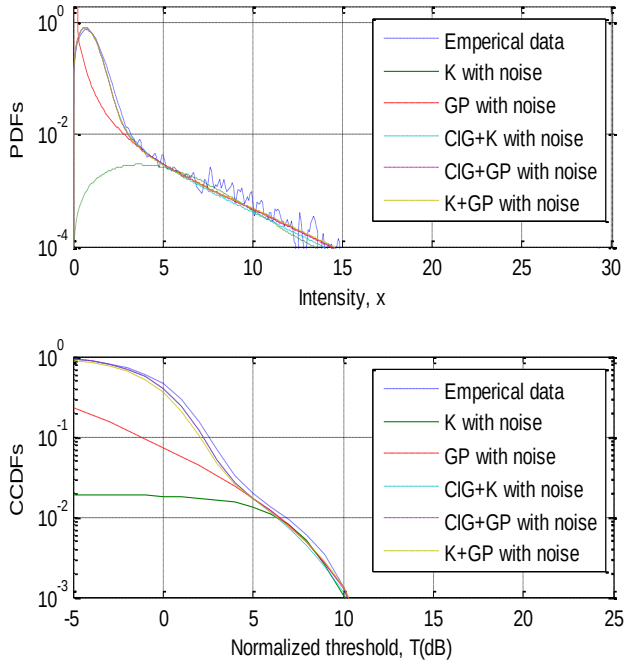

Fig .4: Fitted PDFs and fitted CCDFs of mixture models for HH polarization, resolution of 3m and 17th range cell, dataset 86

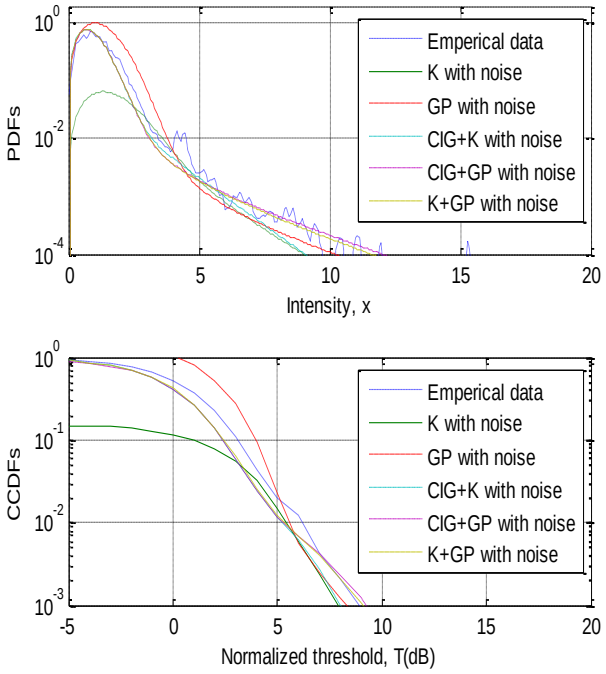

Fig. 5: Fitted PDFs and fitted CCDFs of mixture models for VV polarization, resolution of 3m and 9th range cell, dataset 86

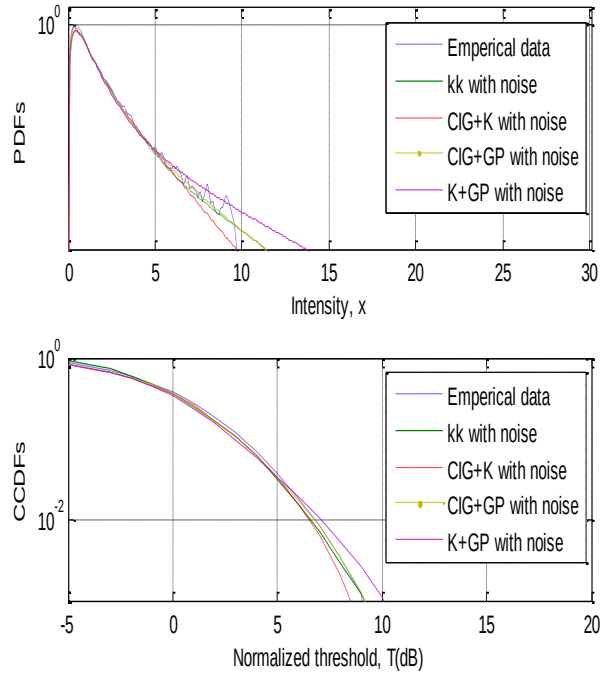

Fig. 6: Fitted PDFs and fitted CCDFs of mixture models for VV polarization, resolution of 30m and 19th range cell, dataset 84

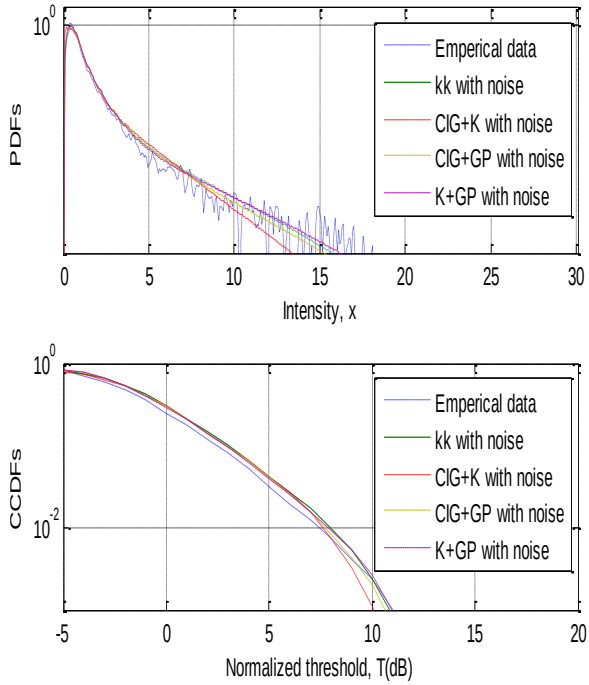

Fig. 7: Fitted PDFs and fitted CCDFs of mixture models for HH polarization, resolution of 15m and 10th range cell, dataset 85

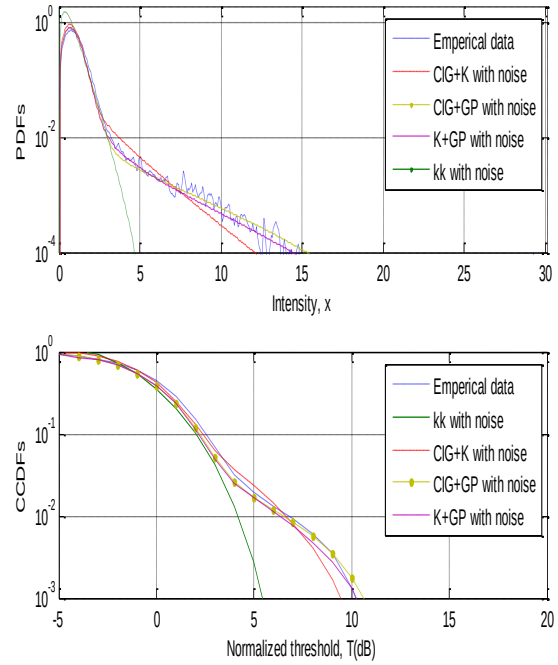

Fig. 8: Fitted PDFs and fitted CCDFs of mixture models for HH polarization, resolution of 3m and 17th range cell, dataset 86

If the HH polarization is used with resolution of 15m and the 10th range cell, all proposed models with noise as shown in Figure 7 overcome the KK model and achieve almost the same tail fitting to

real data with a slight superiority of the CIG plus K that is illustrated by the smallest value of the MSE (Table 3). Now, in the case of a resolution of 3m, HH polarization and 17th range cell, the estimated CIG plus GP CCDF as presented in Figure 8 offers a goodness of fit compared to the obtained KK curve.

Table 1. Estimated parameters of K and Pareto plus noise models for HH and VV polarizations

Distribution	Parameter	HH 30m 19th cell	VV 15m 32th cell	HH 3m 17th cell	VV 3m 9th cell
K+noise	$\hat{\nu}$	0.2599	0.1311	0.1000	0.1000
	$\hat{b}$	0.1105	0.0967	0.072	0.170
	$\hat{\sigma}$	0.1000	0.1000	0.316	0.737
	MSE (dB)	**-5.5221**	**-6.144**	**-5.758**	**-4.848**
Pareto+noise	$\hat{\alpha}$	1.1005	0.1189	7.126	0.237
	$\hat{\beta}$	0.1205	0.0819	0.292	0.477
	$\hat{\sigma}$	0.0954	0.4403	0.472	0.658
	MSE (dB)	**-5.2537**	**-6.1455**	**-5.771**	**-4.803**

Table 2. Estimated parameters of mixture models for HH and VV polarizations

Distribution	Parameters	HH 30m 19th cell	VV 15m 32th cell	HH 3m 17th cell	VV 3m 9th cell
CIG+K with noise	$\hat{\lambda}$	0.4855	1.6354	1.0725	0.1000
	$\hat{\mu}$	15.6892	0.9238	0.5922	1.3673
	κ	0.6466	0.2343	0.9757	0.0000
	$\hat{\nu}$	0.4087	0.1189	7.1264	0.2376
	$\hat{b}$	0.1498	0.0819	0.2921	0.4774
	$\hat{\sigma}$	0.3950	0.4403	0.3616	0.6902
	MSE (dB)	**-6.4875**	**-5.6832**	**-5.643**	**-4.878**
CIG+GP with noise	$\hat{\lambda}$	0.5370	0.8444	0.9649	0.9483
	$\hat{\mu}$	0.7762	2.7913	0.7570	0.8067
	κ	0.5259	0.1053	0.0000	0.7068
	$\hat{\alpha}$	0.7278	1.2668	1.5067	0.7037
	$\hat{\beta}$	0.8462	0.6443	0.4164	0.6455
	$\hat{\sigma}$	0.1000	0.2500	0.2711	0.2477
	MSE (dB)	**-6.1485**	**-6.2621**	**-5.893**	**-5.031**
K+GP with noise	$\hat{\nu}$	0.2990	0.1000	0.2911	0.1583
	$\hat{b}$	1.9826	0.3699	0.7736	0.0723
	κ	0.4407	0.0151	0.0000	0.1601
	$\hat{\alpha}$	0.8815	1.2490	1.4422	2.8539
	$\hat{\beta}$	1.0000	0.6774	0.3532	1.0000
	$\hat{\sigma}$	0.1384	0.2269	0.5641	0.5561
	MSE (dB)	**-5.6246**	**-6.2348**	**-5.878**	**-5.035**

Table 3. Estimated parameters of mixture models for HH and VV polarizations

Distribution	Parameters	VV 30m 19th cell	HH 15m 10th cell	HH 3m 17th cell
K+K With noise	$\hat{\nu}$	1.1460	0.1254	0.1000
	$\hat{b}$	0.2147	0.0551	0.0565
	κ	0.8358	0.2957	0.5111
	$\hat{\nu}_1$	1.5717	0.8931	0.1000
	$\hat{b}_1$	1.0000	0.5739	0.5399
	$\hat{\sigma}$	0.0460	0.3859	0.6222
	MSE (dB)	**-5.7088**	**-5.447**	**-4.218**
CIG+K with noise	$\hat{\lambda}$	0.9362	1.1341	1.3046
	$\hat{\mu}$	1.1664	0.7402	0.1284
	κ	0.8358	0.2957	0.5111
	$\hat{\nu}$	1.1460	0.1254	0.1000
	$\hat{b}$	0.2147	0.0551	0.0565
	$\hat{\sigma}$	0.0460	0.3859	0.6222
	MSE (dB)	**-5.5441**	**-5.7499**	**-5.675**
CIG+GP with noise	$\hat{\lambda}$	0.8729	0.9962	1.1072
	$\hat{\mu}$	2.4484	0.1109	0.5352
	κ	0.5220	0.3889	0.8789
	$\hat{\alpha}$	1.5717	0.8931	0.1000
	$\hat{\beta}$	1.0000	0.5739	0.5399
	$\hat{\sigma}$	0.0672	0.3206	0.5087
	MSE (dB)	**-7.2766**	**-5.748**	**-6.380**
K+GP with noise	$\hat{\nu}$	0.4945	0.3440	0.2704
	$\hat{b}$	1.0225	0.7993	2.5918
	κ	0.3426	0.7225	0.9023
	$\hat{\alpha}$	1.2171	0.7481	0.4520
	$\hat{\beta}$	1.0000	1.0000	0.5358
	$\hat{\sigma}$	0.2181	0.3536	0.6688
	MSE (dB)	**-5.5134**	**-5.510**	**-5.805**

5 Conclusion

The modeling of high resolution sea clutter has been discussed and the mixture distribution with different random textures has been proposed. The additive thermal noise has been incorporated to provide an appropriate model for sea clutter statistics collected by IPIX X-band radar. The proposed model is based on the sum/mixture of two different compound Gaussian distributions plus noise. First, the CIG the *K* and the Pareto plus noise distributions were combined to achieve better tail fitting. Then, unknown parameters were acquired by means of the PCFE method based on the N-M algorithm. Using experimental data, the proposed models can quickly produce satisfactory curve fitting results in most cases compared with standard *K* plus noise, Pareto plus noise, and KK plus noise models. The only drawback of the new mixture models lies in the computational requirements due to the numerical computation of unknown parameters.

References:

[1] Billingsley, J.B., Farina, A., Gini, F., Greco, M.V., Verrazzani, L, Statistical Analyses of Measured Radar Ground Clutter Data. *IEEE Trans. Aerosp. Electron. Syst.*, Vol. 35, no. 2, pp. 597-593, 1999.

[2] Jahangi, M., Blacknell, D., White, R.G, "Accurate approximation to the optimum parameter estimate for K-distributed clutter". *IEE Proc-Radar, Sonar Navig.* Vol. 143, no. 6, pp. 383-390, 1996.

[3] Balleri, A., Nehorai, A., Wang, J, "Maximum likelihood estimation for compound-Gaussian clutter with inverse gamma texture". *IEEE Trans. Aerosp. Electron. Syst.* Vol. 43, no. 2, pp. 775-779, 2007.

[4] Ollila, E., Tyler, D. E., Koivunen, V., Poor, V "Compound-Gaussian Clutter Modeling with an Inverse Gaussian texture distribution". *IEEE Trans. Signal Process. Letter.* Vol. 19, no. 12, pp. 876-879, 2012.

[5] Mezache, A., Chalabi, I., Soltani, F., Sahed, M, "Estimating the Pareto plus noise distribution parameters using non-integer order moments and [zlog(z)] approaches". *IET Radar. Sonar. Navig.* Vol. 10, no. 1, pp. 192-204, 2016.

[6] Mezache, A., Sahed, M., Soltani, F., Chalabi, I, "Model for non Rayleigh Clutter Amplitudes Using Compound Inverse Gaussian Distribution: an experimental analysis". *IEEE Trans. Aerosp. Electron. Syst.* Vol. 51, no. 1, pp. 142-153, 2015.

[7] Alexopoulos, A., Weinberg, G. V, "Fractional order Pareto distributions with application to X-band maritime radar clutter". *IET Radar Sonar Navig.* Vol. 9, no. 7, pp. 817-826, 2015.

[8] Rosenberg, L., Crisp, D. J., Stacy, N.J, "Analysis of the KK-distribution with medium grazing angle sea-clutter". *IET Rad. Son. Navig.* Vol. 4, no. 2, pp. 209-222, 2010.

[9] Abraham, D. A., Gelb, J.M., Oldag, A. W "K-Rayleigh Mixture Model for Sparse Active Sonar Clutter". OCEANS '10 *IEEE Conference,* 24-27 May, Sydney, NSW, 2010

[10] Zhou, X., Peng, R., Wang, "A Two-Component K–Lognormal Mixture Model and Its Parameter Estimation Method". *IEEE Trans. on Geos. remote. sens.* Vol. 53, no. 5, pp. 2640-2651, 2015.

[11] A. Gouri, A. Mezache, H. Oudira, A. Bentoumi, "Mixture of Compound-Gaussian Distributions for Radar Sea-Clutter Modeling ", In *Proceedings of the IEEE 2016 International Conference on Control Engineering & Information Technology, December 16-18, 2016*, Hammamet, Tunisia

[12] A. Mezache, M. Sahed, T. Laroussi, D. Chicouche, 'Two novel methods for estimating the compound K-clutter parameters in presence of thermal noise', *IET Radar Sonar Navig*., 2011, vol. 5, no. 9, pp. 934-942, 2011.

[13] Ward, K. D., Tough, R J.A., Watts, S.: 'Sea Clutter: Scattering, the K-distribution, and Radar Performance', *Second edition IET, London, UK*, 2013

[14] A. Mezache, I. Chalabi, T. Laroussi, M. Sahed,: 'K-clutter plus noise parameter estimation using fractional positive and negative moments', *IEEE Trans. Aerosp. Electron. Syst,* vol. 52, no. 2, pp. 960-967, 2016.

[15] L. Rosenberg, S. Bocquet,: 'The Pareto distribution for high grazing angle sea-clutter', *IEEE Int. Geoscience and Remote Sensing Conf.,* 21-26 July 2013, Melbourne, Australia

[16] S. Bocquet,: 'Parameter estimation for Pareto and K distributed clutter with noise,' *IET Radar. Sonar. Navig.,* vol. 9, no. 1, pp. 104-113, 2014.

[17] M. Sahed, A. Mezache,: 'Closed-form estimators for the Pareto clutter plus noise parameters based on non-integer positive and negative order moments', *IET Radar Sonar Navig,* vol. 11, no. 2, pp. 359-369, 2017.

[18] A. Mezache, A. Bentoumi, M. Sahed,: 'Parameter Estimation for Compound-Gaussian Clutter with Inverse-Gaussian Texture', *IET Rad. Son. Navig.*, vol. 11, no. 4, pp. 586-596, 2017.

[19] V. Seshadri,: 'The Inverse Gaussian Distribution- Statistical Theory and Applications', *Springer Science* 1999.

[20] R. Bakker and B. Currie, "The McMaster IPIX radar sea clutter database", 2001, [Online]. Available: http://soma.mcmaster.ca/ipix/ (Accessed Date: December 19, 2023).

Contribution of Individual Authors to the Creation of a Scientific Article (Ghostwriting Policy)

- The research project was led by Houcine Oudira, who supervised the simulation, algorithm implementation, paper preparation and review, and paper editing.
- Amar Mezache and Amel Gouri carried out the writing, reviewing, and editing of the paper.

Sources of Funding for Research Presented in a Scientific Article or Scientific Article Itself

No funding was received for conducting this study.

Conflict of Interest

The authors have no conflicts of interest to declare.